Journal for ImmunoTherapy of Cancer

Assessing the implications of sentinel lymph node removal in cervical cancer: an immunogenetic perspective – a SENTICOL ancillary study

Gaurav Thareja ,[1] Anna Salvioni,[2] Françoise Lauzeral-Vizcaino,[3] Najeeb Halabi,[1] Eliane Mery-Lamarche,[4] Noemie Thebault,[3] Clara-Maria Scarlata,[3] Marie Michelas,[3] Anne-Sophie Navarro,[5] Gwenaël Ferron,[3,5] Fabrice Lecuru,[6,7] Patrice Mathevet,[8] Jonathan Khalifa,[3,9] Maha Ayyoub,[3] Arash Rafii,[10] Alejandra Martinez[3,5,11]

To cite: Thareja G, Salvioni A, Lauzeral-Vizcaino F, *et al*. Assessing the implications of sentinel lymph node removal in cervical cancer: an immunogenetic perspective – a SENTICOL ancillary study. *Journal for ImmunoTherapy of Cancer* 2024;**12**:e008734. doi:10.1136/jitc-2023-008734

► Additional supplemental material is published online only. To view, please visit the journal online (https://doi.org/10.1136/jitc-2023-008734).

GT and AS are joint first authors.

Accepted 01 May 2024

For numbered affiliations see end of article.

Correspondence to
Prof Alejandra Martinez; martinez.alejandra@iuct-oncopole.fr

ABSTRACT

Background Cervical cancer's lymphatic spread primarily begins from the sentinel lymph nodes (SLNs), underlining their pivotal role in disease metastasis. However, these nodes' immune gene expression profiles and immunoregulation mechanisms have yet to be explored.

Methods Our study aimed to elucidate the immune cell populations and their roles in the immune gene expression profile of negative SLNs compared with positive SLNs and non-SLNs using Nanostring RNA seq analysis. We performed a principal component analysis on the log2 normalized expression of 685 endogenous genes in the nCounter PanCancer Immune Profiling Panel, followed by an assessment of the differential expression of genes and immune cell type abundance.

Results We found significant variations in gene expression among the groups, with negative SLNs displaying overexpression of genes related to tumor-infiltrating immune cells, specifically innate cell populations. They also demonstrated the upregulation of genes involved in antigen presentation and T-cell priming. In contrast, positive SLNs were enriched in regulatory networks, suggesting their potential role in immune evasion. A comparison of negative SLNs and non-SLNs revealed increased innate and adaptive immune cell types, underscoring the ongoing T cell response to tumor antigens.

Conclusion Our findings underscore a specific immunogenetic phenotype profile in negative SLNs, emphasizing their crucial role in the initial anticancer response, immunosurveillance, and the propagation of immune tolerance from the primary cervical tumor. These results highlight the potential of SLNs as a novel target for immunotherapy strategies and underscore the importance of new imaging methods for accurately identifying SLN status without removal. Future investigations are needed to understand further the immunological interplay within SLNs and their influence on cervical cancer progression.

WHAT IS ALREADY KNOWN ON THIS TOPIC

⇒ The sentinel lymph node (SLN) plays an important role in immunosurveillance but is often surgically removed to profile lymph node involvement in primary cervical cancer.

WHAT THIS STUDY ADDS

⇒ We applied the nCounter PanCancer Immune Profiling panel on 36 SLN biopsies were obtained, comprising 12 metastatic SLNs, 12 negative SLNs, and their corresponding paired non-SLNs from 24 patients.

⇒ We identified differentially expressed genes characteristic of negative SLNs compared with the other two groups. The negative SLNs are enriched with genes involved in T-cell priming and antigen presentation.

HOW THIS STUDY MIGHT AFFECT RESEARCH, PRACTICE OR POLICY

⇒ Our study identified the active immunosurveillance role of negative SLN in early-stage cervical cancer patients. Therefore, new methodologies are required for staging cancer patients rather than SLN removal, as SLNs could control antitumor immune response.

BACKGROUND

Cervical cancer remains a significant global health issue, ranking as one of the most prevalent malignant diseases and leading causes of mortality among women worldwide.[1 2] Despite its high curability when detected in early stages, survival rates plummet substantially when lymph nodes become involved, emphasizing the significance of lymph node involvement as a primary prognostic factor.[3] Sentinel lymph node (SLN) detection has proven to be an accurate method for identifying lymph node involvement in early-stage cervical cancer.[4–6] The SLN represents the first interaction between tumor antigens and the adaptive immune response, potentially the initial site for eliciting antitumor adaptive responses that could contribute to tumor dissemination. Furthermore, SLNs

undergo unique molecular and structural alterations, facilitating metastasis via the lymphatic system to distant sites.[7]

The molecular signals and cellular changes that underlie lymph node metastasis in cervical cancer remain underexplored.[8 9] In contrast, several developments such as lymphangiogenesis, heightened lymph flow, the recruitment and proliferation of immunosuppressive cells, upregulation of chemokines and cytokines, vascular remodeling, and a reduction in the proportion of effector T cells have been characterized in patients with breast cancer.[10] Melanoma research demonstrates that tumor-induced immunosuppression in SLNs precedes and promotes metastasis to regional lymph nodes. Enlarged suppressive populations and shifts in T cell phenotypes have been identified in SLNs compared with non-SLNs in patients with melanoma. Immunohistochemical analyses reveal a shift in T-cell polarity within the paracortex of the lymph nodes, characterized by an increase in Th2, a decrease in Th1 and CD8 populations, and diminished infiltration of dendritic cells between SLNs and control nodes. Several factors, such as the downregulation of CD62L that retains T-cells within the lymph node to promote antigen presentation, costimulation, and T-cell proliferation, have been linked with hindered T-cell trafficking in the SLNs of melanoma patients.[11] Additional studies reveal that the increase in Th2 polarization and decrease in Th1 populations observed in SLNs are associated with elevated Th2 polarizing cytokines (TNFα) and a decline in Th1 polarizing cytokines (IFN and IL-12B).[12 13] Increased expression of immune checkpoints such as PD-1 and CTLA4 has also been discovered in CD8 T-cells located in SLNs, resulting in impaired T-cell proliferation and cytokine production.[14 15] These findings, among others, underscore the potential of immune signatures in SLNs as indicators of disease progression.[16]

The majority of research efforts have focused on the correlation between molecular characteristics of cervical tumors and patient survival or the relationship between cervical tumor gene expression profiles and lymph node involvement.[17] However, the functional role of immune infiltration within lymph nodes and the mechanisms that lead to lymphocyte functional impairment within SLNs in cervical cancer remain inadequately studied. These aspects are crucial for understanding the intricacies of lymph node metastasis and the propagation of the disease. Tools like Nanostring nCounter PanCancer Immune Profiling Panel facilitate a comprehensive immune analysis of lymph nodes, enabling the identification of immunological distinctions between adjacent lymph nodes.[18] Our study aims to delve into the immune cell populations and the mechanisms of immunoregulation involved in the immune gene expression profile of negative SLNs in cervical cancer compared with positive SLNs and non-SLNs.

METHODS

Patients and tissue specimens

24 consecutive cervical cancer cases from patients in the SENTICOL I and II (NCT01639820) studies and in the DECIDE protocol (NCT03958240) at the Institut Universitaire du Cancer in Toulouse were included in the study group. Patients were selected when clinical data were available, and SLN was larger than 1 cm to avoid using all the formalin-fixed paraffin embedded (FFPE) bloc. The sample size was predefined to compare 12 positive SLNs with 12 negative SLNs and their paired non-SLNs. Patients were being treated according to ESGO (European Society of Gynaecological Oncology) guidelines when clinical data were extracted.

RNA extraction from FFPE tissue

According to the surface of the tumor area, 3–8 tissue sections of 10 µm were cut from each selected block using an RNase-free microtome and collected in RNase-free tubes. RNA was extracted as soon as possible after sectioning. Deparaffinization of the samples was performed with the Qiagen Deparaffinization Solution (Qiagen, Germany, Cat#19093), and total RNA was extracted by applying the Qiagen RNeasy FFPE kit (Qiagen, Hilden, Germany, Cat#73504). RNA concentration was quantified by NanoDrop and Qubit Fluorometer. The RNA quality was analyzed using the Agilent Fragment Analyzer System.

NanoString gene expression profiling

Immune gene expression analysis was performed with the NanoString nCounter analysis system (NanoString Technologies, Seattle, Washington, USA) using the commercially available nCounter PanCancer Immune Profiling panel kit. The PanCancer Immune profiling panel contains 730 genes of key inflammatory pathways and 40 reference genes covering both innate and adaptive immune responses. According to the state of RNA degradation, the manufacturer's protocol was modified, and total RNA extracted from biopsies was hybridized with probes at 65°C for 16 hours. Samples were processed on the NanoString Prep Station, and the target-probe complex was immobilized onto the analysis cartridge. Cartridges were scanned by the nCounter Digital Analyser for digital counting of molecular barcodes corresponding to each target at 490 fields of view.

Data analysis

The data were analyzed using nSolver Analysis Software V.4.0 and nSolver Advanced Analysis Module with NS_CancerImmune_V1.1 codeset. The raw data from all samples were imported into the analysis software using default options. Data were normalized using the background thresholding to the geometric mean of the negative control probes; positive control probes were further used for intersample normalization. Finally, the geometric mean of the housekeeping genes was used to normalize for analyte abundance. After extensive QC steps, data

were imported into the advanced analysis module and was not again normalized for differential expression, pathway scoring, and cell-type profiling.

Statistical analysis

The principal component analysis (PCA) was computed on normalized counts of 685 genes using the prcomp function in R V.4.2.3 with centering and scaling of the data. The cell type abundance and pathway scores were compared between groups using t-tests, and a $p<0.05$ was considered significant. The genes with FDR (False Discovery Rate) $p<0.05$ and $\log_2FC>|\pm 1.5|$ from the differential gene expression analysis were considered significant. The gene annotations for significantly differentially expressed genes were extracted from Ingenuity Pathway Analysis.

The DE, cell-type, and pathway analysis figures were generated using EnhancedVolcano and ggplot2 packages in R V.4.2.3.[19 20]

RESULTS

FFPE blocks from a total of 36 samples were obtained, comprising 12 metastatic SLNs, 12 negative SLNs, and their corresponding paired non-SLNs from 24 patients, all of which were included in the study. Total RNA was extracted from these samples, and transcriptomics profiling was performed, in each sample, using nCounter PanCancer Immune Profiling Panel (NanoString technology) (online supplemental table 1 provides all experimental QC details). A set of ix samples had a binding density measure outside the default range. However, as there were no other QC parameters outside the default range for these samples, these samples were included in the analysis. All the samples were normalized together in our study.

PCA captures high immune gene expression variability in the negative SLN group

We conducted PCA on the $\log_2$ normalized expressions of 685 endogenous genes featured in the nCounter PanCancer Immune Profiling Panel. The first principal component (PC1), which accounts for 40.51% of the total variance, effectively distinguished negative SLNs from Positive SLNs and non-SLN groups, as depicted in figure 1A,B. The second and third PC (PC2 and PC3) could differentiate between the Positive SLN and non-SLN groups, as shown in figure 1C,D. Intriguingly, four samples from the Negative SLN group clustered with

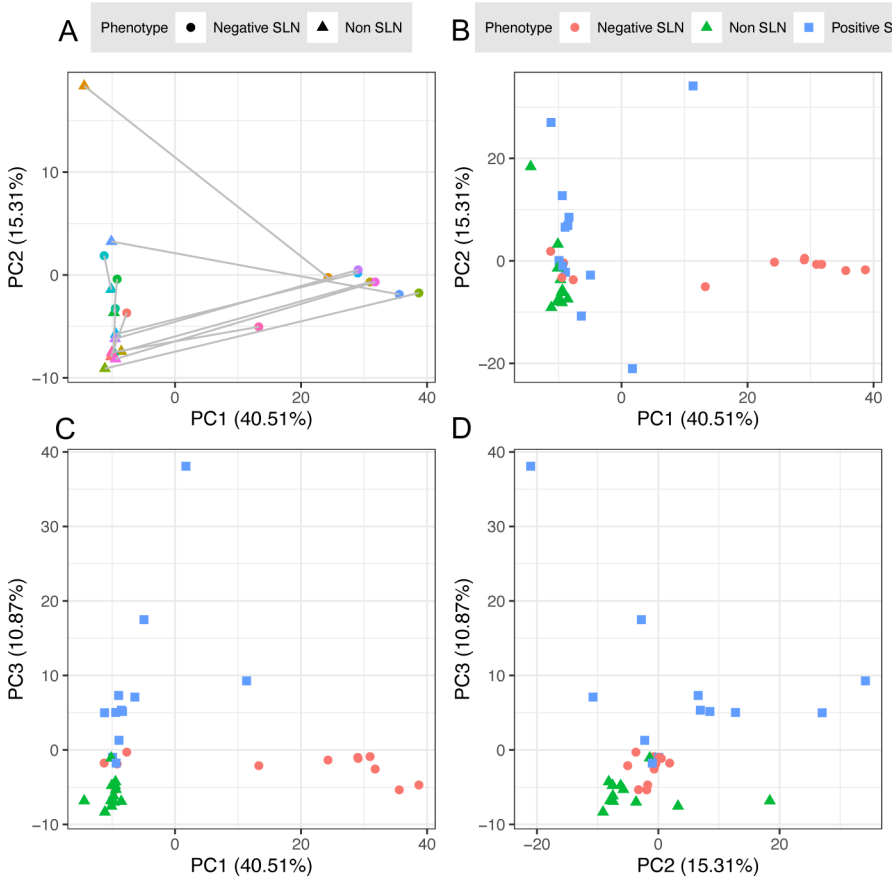

Figure 1 Principal component analysis (PCA) illustrating the heterogeneity in gene expression across different lymph nodes involved in various stages of cancer progression. (A) When paired, the negative sentinel lymph nodes (SLNs) and non-SLNs form distinct clusters. The PCA plots highlight that the negative SLNs exhibit the highest variability in immune gene expression compared to the other two lymph node groups. Moreover, the principal components further delineate these different lymph node groups.

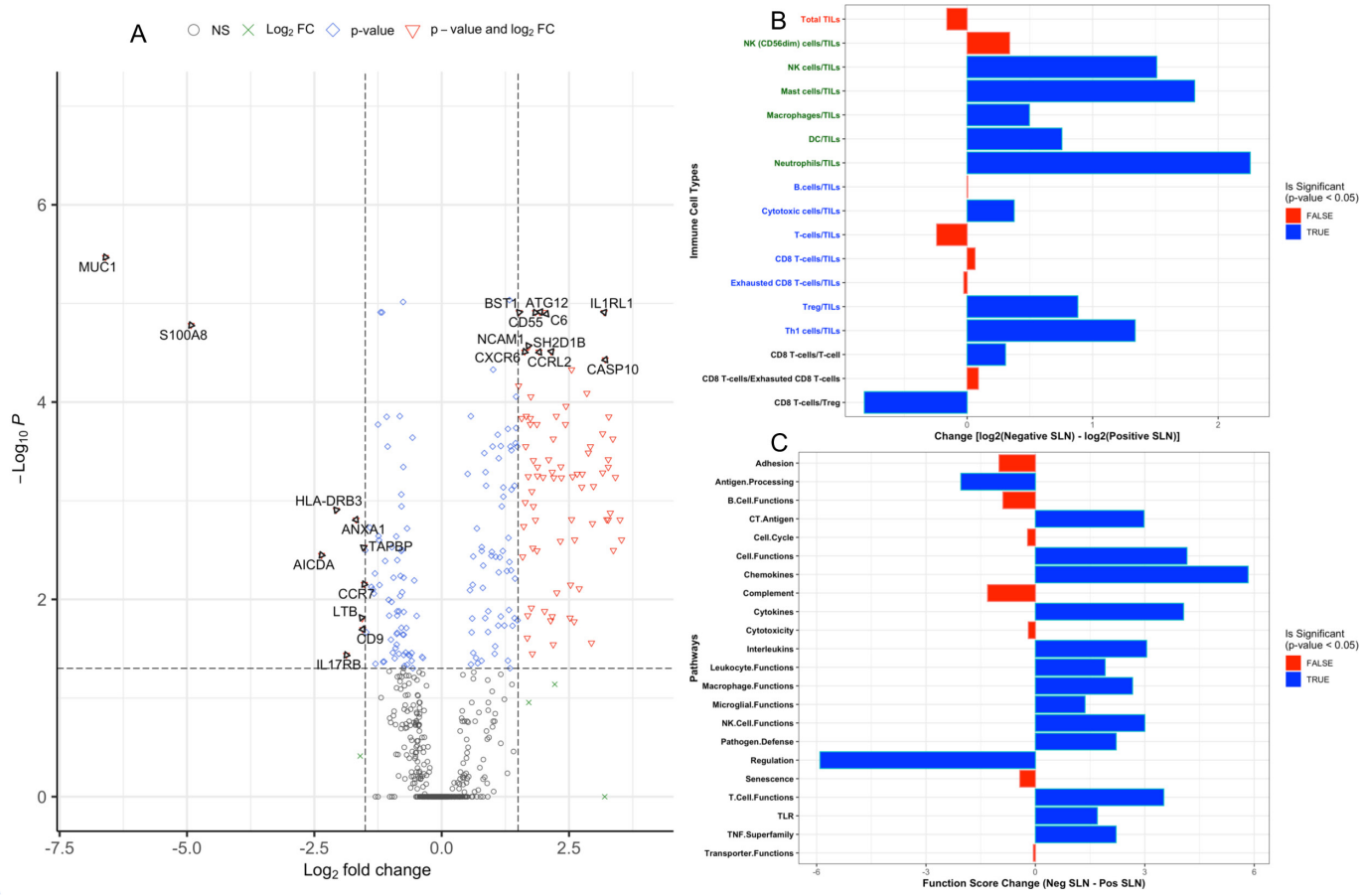

Figure 2 Differential gene expression analysis between negative sentinel lymph nodes (SLNs) and positive SLNs. (A) A volcano plot depicts the upregulated and downregulated genes with a log2 fold-change greater than |±1.5| in negative SLNs compared with positive SLNs. (B, C) The relative abundance of various immune cell types and pathways, as determined through gene enrichment analysis, emphasizes their differential activity based on the SLN status.

those from the positive and non-SLN groups. Despite thorough examination, none of the available clinical and technical parameters could discriminate these outlier samples from those in the negative SLN group.

Negative SLN are enriched in innate immune cells as compared with positive SLN group

We conducted a comparative analysis of gene expression, immune cell type abundance, and inferred functional pathways between the Negative SLN group and the Positive SLN group using the nSolver Advanced Analysis Module. This examination revealed a significant differential expression of 90 genes between the groups, adhering to a Benjamini-Yekutiel $p<0.05$ and a $\log_2$ fold change>|±1.5| (figure 2A—depicting a volcano plot of differentially expressed genes). Among these 90 genes, 80 were upregulated, and 10 were downregulated (table 1—presenting the top 10 significantly downregulated and upregulated genes; online supplemental table 3 enumerates the comprehensive differential expression results).

Immune cell type deconvolution did not highlight statistically significant differences in the total infiltrating lymphocytes. However, we noted a statistically significant increase in the relative abundance of most innate immune cell types in Negative SLNs compared with Positive SLNs (figure 2B—showing a bar chart of the relative abundance of inferred cell types). An increase was also observed in the relative abundance of Tregs and Th1 helper T cells in Negative SLNs relative to positive SLNs. No significant reductions were detected in any of the innate and adaptive immune system cell types in negative SLNs compared with positive SLNs, suggesting an active role for negative SLNs in immune editing.

Lastly, pathway functional scores were estimated to assess the up-and-down activity of immune-related pathways. We discerned that the majority of pathways displayed increased activity in negative SLNs compared with positive SLNs, with the chemokines secretion pathway presenting the highest positive activity. Conversely, a high negative activity was observed in the regulation pathway, which incorporates genes involved in diverse regulatory processes such as the cell cycle and cellular adhesion (figure 2C—showing a bar chart of pathway functional score change).

Negative SLNs have a high abundance of all types of immune cells compared with non-SLNs

A differential expression comparison between the negative SLN group and the non-SLN group identified a total of 93 differentially expressed genes, adhering to a

Table 1 An enumeration of the top 10 upregulated and downregulated genes, ranked by their differential expression between negative sentinel lymph nodes (SLNs) and positive SLNs (the genes are ordered based on their p value)

Gene name	Log2 fold change	P value	By P value	Entrez gene name	Location	Type(s)
CD55	1.84	1.40E–08	1.23E–05	CD55 molecule (Cromer blood group)	Plasma Membrane	Other
C6	2.03	1.92E–08	1.23E–05	Complement C6	Extracellular Space	Other
ATG12	1.93	2.13E–08	1.23E–05	Autophagy related 12	Cytoplasm	Other
IL1RL1	3.19	2.67E–08	1.23E–05	Interleukin 1 receptor like 1	Plasma Membrane	Transmembrane receptor
BST1	1.52	2.72E–08	1.23E–05	Bone marrow stromal cell antigen 1	Plasma Membrane	Enzyme
NCAM1	1.71	7.28E–08	2.73E–05	Neural cell adhesion molecule 1	Plasma Membrane	Other
SH2D1B	2.15	1.00E-07	3.09E-05	SH2 domain containing 1B	Cytoplasm	Other
CXCR6	1.63	1.01E–07	3.09E–05	C-X-C motif chemokine receptor 6	Plasma Membrane	G-protein coupled receptor
CCRL2	1.91	1.03E–07	3.09E–05	C-C motif chemokine receptor like 2	Plasma Membrane	G-protein coupled receptor
CASP10	3.21	1.32E–07	3.71E–05	Caspase 10	Cytoplasm	Peptidase
MUC1	–6.6	7.54E–10	3.40E–06	Mucin 1, cell surface associated	Plasma Membrane	Other
S100A8	–4.92	4.06E–08	1.66E–05	S100 calcium-binding protein A8	Cytoplasm	Other
HLA-DRB3	–2.07	2.43E–05	0.00124	Major histocompatibility complex, class II, DR beta 3	Cytoplasm	Other
ANXA1	–1.68	3.20E–05	0.00156	Annexin A1	Plasma Membrane	Enzyme
TAPBP	–1.52	7.08E–05	0.00295	TAP binding protein	Cytoplasm	Transporter
AICDA	–2.36	9.48E–05	0.00356	Activation-induced cytidine deaminase	Cytoplasm	Enzyme
CCR7	–1.52	0.000216	0.00701	C-C motif chemokine receptor 7	Plasma Membrane	G-protein coupled receptor
LTB	–1.56	0.000593	0.0156	Lymphotoxin beta	Extracellular Space	Cytokine
CD9	–1.55	0.000805	0.0201	CD9 molecule	Plasma Membrane	Other
IL17RB	–1.87	0.00166	0.0366	Interleukin 17 receptor B	Plasma Membrane	Transmembrane receptor

Gene annotations were conducted using Ingenuity Pathway Analysis Software.

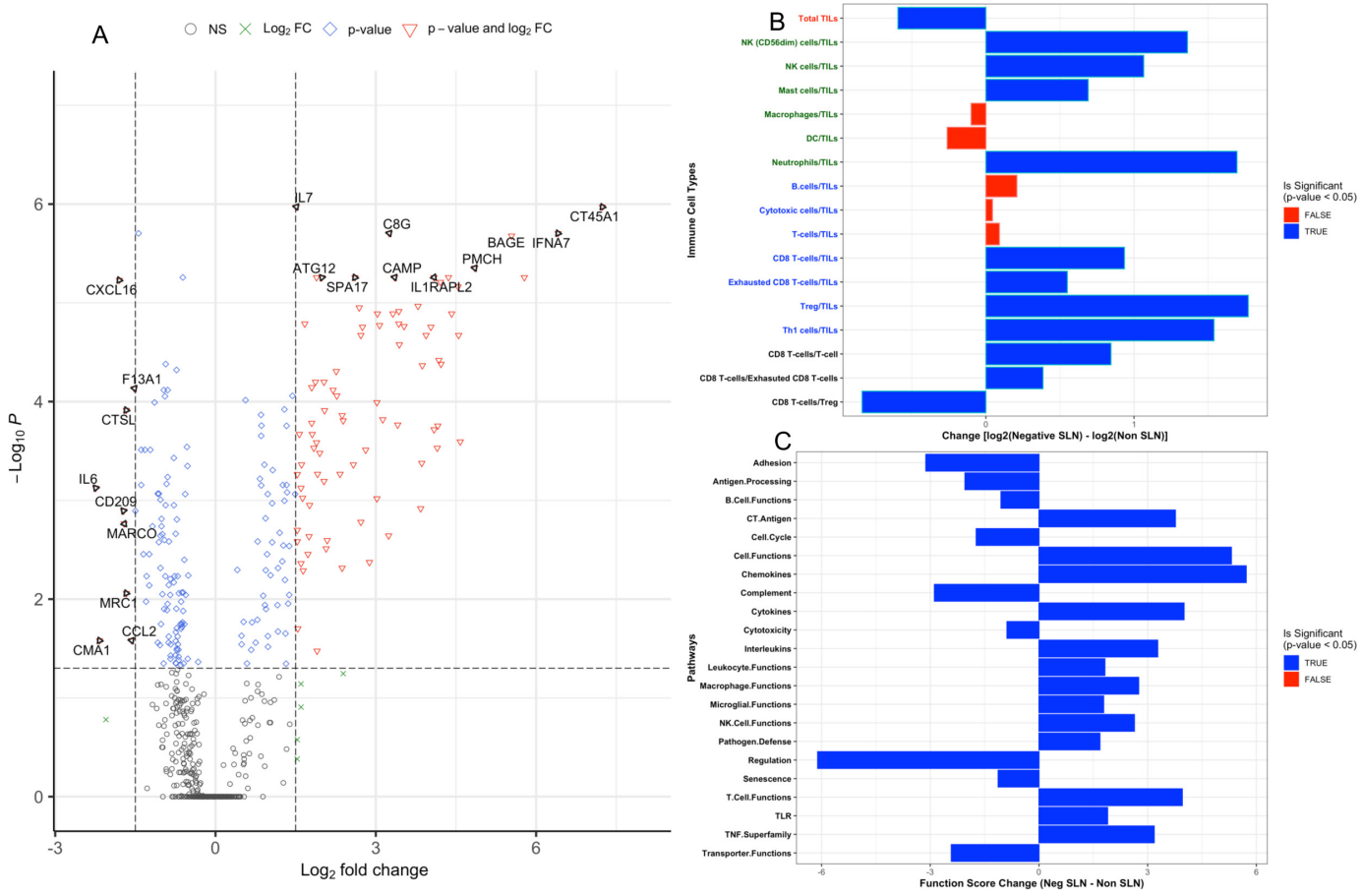

Figure 3 Differential gene expression analysis between negative sentinel lymph nodes (SLNs) and non-SLNs. (A) A volcano plot displays the upregulated and downregulated genes with a log2 fold-change greater than ±1 in negative SLNs compared to non-SLNs. (B, C) The relative abundance of various immune cell types and pathways, as determined through gene enrichment analysis, underlines their differential activity based on the SLN status.

Benjamini-Yekutiel p<0.05 and a $\log_2$ fold change>|±1.5| (figure 3A—illustrating a volcano plot of differentially expressed genes). Among these 93 genes, 84 were upregulated, with only 9 downregulated (table 2—presenting the top 10 significantly downregulated and upregulated genes; online supplemental table 4 provides a complete list of differential expression results).

Interestingly, 56 upregulated genes were shared between both differential expression analyses (negative SLNs vs positive SLNs and negative SLNs vs non-SLNs). In contrast, none of the downregulated genes overlapped between the two comparisons.

The results of immune cell deconvolution revealed a substantial increase in the majority of innate and adaptive immune cell types (figure 3B—showing a bar chart of the relative abundance of inferred cell types). Unlike the comparison between negative SLNs and positive SLNs, we noted a significant uptick in the number of CD8+T cells and exhausted CD8+T cells in the negative SLNs versus non-SLNs comparison. We also recorded a marked reduction in the relative abundance of macrophages and dendritic cells compared with the negative SLNs versus positive SLNs analysis. This observation implies that antigen presentation is a shared feature of both negative SLNs and non-SLNs, but these cells are less abundant in the positive SLN environment.

Lastly, we observed that all pathways significantly differ between negative SLNs and non-SLNs. Similar to the negative SLNs versus positive SLNs analysis, the chemokines pathway showed the highest positive activity, and the regulation pathway showed the highest negative activity. All pathway functional activity score changes were in the same direction as in the negative SLNs versus positive SLNs analysis (figure 3C—showing a bar chart of pathway functional score change).

DISCUSSION

This study delved into the immune gene expression profile of negative SLNs in comparison to metastatic SLNs (positive SLNs) and non-SLNs in cervical cancer. We identified 90 and 93 differentially expressed genes in the negative SLNs versus positive SLNs and negative SLNs versus non-SLN comparisons, respectively. 80 and 84 genes were overexpressed, and 10 and 9 were underexpressed in each comparison. Our findings implicate genes involved in immune evasion, as evidenced by the downregulation of antigen presenting cells (APCs) and

Table 2 An enumeration of the top upregulated and downregulated genes, classified by their differential expression between negative sentinel lymph nodes (SLNs) and non-SLNs

Gene name	Log_2 fold change	P value	By p value	Entrez gene name	Location	Type(s)
IL7	1.51	2.42E−10	1.07E−06	Interleukin 7	Extracellular Space	Cytokine
CT45A1	7.24	4.74E−10	1.07E−06	Cancer/testis antigen family 45 member A2	Other	Other
IFNA7	6.41	1.32E−09	1.98E−06	Interferon alpha 7	Extracellular Space	Cytokine
C8G	3.25	2.00E−09	1.98E−06	Complement C8 gamma chain	Extracellular Space	Transporter
BAGE	5.54	2.80E−09	2.10E−06	B melanoma antigen	Other	Other
PMCH	4.85	6.90E−09	4.44E−06	Pro-melanin concentrating hormone	Extracellular Space	Other
ATG12	1.99	1.18E−08	5.53E−06	Autophagy related 12	Cytoplasm	Other
IL1RAPL2	4.09	1.48E−08	5.53E−06	Interleukin 1 receptor accessory protein like 2	Plasma Membrane	Transmembrane receptor
SPA17	2.61	1.56E−08	5.53E−06	Sperm autoantigenic protein 17	Plasma Membrane	Other
CAMP	3.35	1.63E−08	5.53E−06	Cathelicidin antimicrobial peptide	Cytoplasm	Other
CXCL16	−1.8	2.22E−08	5.89E−06	C-X-C motif chemokine ligand 16	Extracellular Space	Cytokine
F13A1	−1.52	7.36E−07	7.37E−05	Coagulation factor XIII A chain	Extracellular Space	Enzyme
CTSL	−1.67	1.52E−06	0.000122	Cathepsin L	Cytoplasm	Peptidase
IL6	−2.24	1.67E−05	0.00075	Interleukin 6	Extracellular Space	Cytokine
CD209	−1.72	3.31E−05	0.00128	CD209 molecule	Plasma Membrane	Other
MARCO	−1.71	4.65E−05	0.00172	Macrophage receptor with collagenous structure	Plasma Membrane	Transmembrane receptor
MRC1	−1.67	0.00033	0.00873	Mannose receptor C-type 1	Plasma Membrane	Transmembrane receptor
CCL2	−1.57	0.0012	0.0262	C-C motif chemokine ligand 2	Extracellular Space	Cytokine
CMA1	−2.17	0.00121	0.0263	Chymase 1	Extracellular Space	Peptidase

The genes are arranged in order of their p value. Gene annotations were facilitated using the Ingenuity Pathway Analysis Software.

cytotoxic populations in metastatic lymph nodes. In contrast, negative SLNs demonstrated significant variability in gene expression data, with overexpression of genes encoding tumor-infiltrating immune cell populations, particularly innate cell populations, as well as genes involved in antigen presentation and T-cell priming. Network analysis revealed upregulated genes primarily implicated in chemokine, cytokine, and immune innate and T cell functions in negative SLNs while genes in positive SLNs were enriched in regulatory networks.

SLNs are central to tumor antigen-specific lymphocyte priming and play a significant role in cervical cancer's antitumor immunity. Despite this, their potential as a therapeutic target has primarily been underexplored. SLNs, routinely removed for pathology exams, offer valuable insights for staging to adjust treatment strategies.[21–23] Most existing studies have focused on the immune microenvironment of metastatic lymph nodes, describing an enrichment of immunosuppressive cell subsets and increased expression of immune checkpoints.[10 24] However, it remains crucial to understand the immunological impact of removing tumor-draining lymph nodes and whether it resembles removing metastatic lymph nodes from negative SLNs or regional lymph nodes.

Our results unveil a unique immunogenetic phenotype profile in negative SLNs, hinting at their pivotal role in the initial anticancer response, immunosurveillance, and the propagation of immune tolerance from the cervical tumor. The key takeaway is that negative SLNs exhibit pronounced upregulation of innate immune activators, leading to an enhanced IFN type-I response to boost the T cell infiltration.[25] Moreover, non-invaded SLNs showed increased expression of genes coding for APCs, especially neutrophils, and upregulated genes implicated in antigen presentation and cytotoxic Th1 responses compared with metastatic SLNs. Regulation pathways involved in immune evasion are upregulated in metastatic SLNs.[26]

Examining individual genes, we noticed an upregulation of CXCR6 in negative SLNs compared with metastatic SLNs. CXCR6 aids the survival of effector T cells within the tumor microenvironment, supports perivascular CD3 to boost cytotoxic T lymphocyte (CTL) infiltration and has been linked with favorable prognostic outcomes in cervical and other cancers.[27 28]

Interestingly, negative SLNs showed enrichment in exhausted CD8 T and Th1 cells compared with non-SLNs, indicating an ongoing specific T cell response to tumor antigens. This enrichment, considered an indirect marker of T cell-specific activity, is consistent with earlier findings, where lower CD8 T cell/Treg ratios were observed in positive LNs compared with negative LNs.[8 29 30] Further investigations are needed to validate these findings and understand the therapeutic potential of the SLN, especially in the context of immunotherapy strategies. The clinical question is to understand how the removal of SLNs might affect the long-term immune response in patients and how to target SLNs. From a surgical perspective, metastatic lymph nodes present an immunosuppressive microenvironment similar to a primary tumor, and surgical resection may help or not impair locoregional immune control. On the contrary, negative SLN is an immune hotspot and the first step for the initiation of the specific T cell response. Future perspectives include assessing whether SLN can be a specific target for immunotherapy strategies, and we propose that immunotherapy neoadjuvant strategies may enhance priming and increase T cell antitumor response. In support of this hypothesis, a phase II trial comparing neoadjuvant to adjuvant pembrolizumab in patients with stages III–IV resectable melanoma demonstrated a significant increase in 2-year disease-free survival among patients treated with the neoadjuvant strategy.[31] Although melanoma is recognized as a more immunogenic disease with higher response rates to immunotherapy compared with cervical cancer, this study highlights the potential role of lymph nodes in the antitumor immunological response. Specifically, it suggests a higher response to immunotherapy when lymph nodes have not been surgically removed. Finally, developing sensitive imaging methods for SLN status determination without node removal should also be explored.

The sample size and the missing biopsies of the primary tumors limit the study. Genetic changes can influence the tumor microenvironment in the cancer cells; therefore, it is important to understand their role in modifying the immune landscape of SLNs. We observed four negative SLN biopsies clustering with other lymph node biopsies, indicating some other factor playing a role that cannot be deciphered from routine clinical measurements.

CONCLUSION

Our research underscores the fundamental role of SLN as the primary site of metastasis in cervical cancer. From our study, it is evident that the SLN significantly hinders the lymphatic dissemination of cervical cancer. We observed notable immunological alterations within the SLN compared with its non-SLN counterparts. Furthermore, we identified an enrichment of innate and T cell transcripts within the immune gene expression profile of a negative SLN, suggesting it provides an environment conducive to the onset of an adaptive immune response. Intriguingly, our findings also indicate that changes in SLN-related transcripts favor tolerance, thereby establishing a premetastatic niche that could potentially facilitate lymph node invasion.

Author affiliations
[1]Weill Cornell Medicine, Doha, Qatar
[2]Centre de recherche en cancerologie de Toulouse, Toulouse, France
[3]Centre de Recherches en Cancérologie de Toulouse INSERM UMR1037, Toulouse, France
[4]Pathology Department, Oncopole Claudius Regaud, Institut Universitaire du Cancer Toulouse Oncopole, Toulouse, France
[5]Surgical Oncology Department, Oncopole Claudius Regaud, Institut Universitaire du Cancer Toulouse Oncopole, Toulouse, France
[6]Gynecologic Oncology Department, Institut Curie, Paris, France
[7]Paris Cité University, Paris, France
[8]Gynecology Department, Centre Hospitalier Universitaire Vaudois, Lausanne, Switzerland
[9]Radiotherapy Department, Oncopole Claudius Regaud, Institut Universitaire du Cancer Toulouse Oncopole, Toulouse, France

[10]ScieNFT, Paris, France
[11]Toulouse III-Paul Sabatier University, Toulouse, France

Acknowledgements GT is supported by the Biomedical Research Program at Weill Cornell Medicine in Qatar, a program funded by the Qatar Foundation.

Contributors AM and AR designed and supervised the study. AS conducted the experiments. GT, NH, and AR analyzed the data. FL-V, EM-L, NT, CM-S, MM, A-SN, GF, FL, PM, JK and MA provided materials. AM, AR, and GT wrote the manuscript. All authors approved the final version of the manuscript. AM acts as guarantor for this manuscript.

Funding Financial support: SENTICOL I and II studies were financially supported by the French National Cancer Institute (STIC 2008 and 2012).

Competing interests None declared.

Patient consent for publication Not applicable.

Ethics approval This study involves human participants and SENTICOL I, II, and DECIDE studies were approved by the Comite de Protection des Personnes Sud-Est IV, 2008-A01369-46; Comite´ de Protection des Personnes, HEGP-Broussais DRRC AOR 03063; and DC-2016-2656. All patients provided written informed consent before inclusion. Participants gave informed consent to participate in the study before taking part.

Provenance and peer review Not commissioned; externally peer reviewed.

Data availability statement Data are available on reasonable request. Raw Data are available on reasonable request. All data relevant to the study are included in the article or uploaded as online supplemental information.

ORCID iD
Gaurav Thareja http://orcid.org/0000-0003-2277-6400

REFERENCES

1 Cancer STAT facts: cervical cancer. n.d. Available: https://seer.cancer.gov/statfacts/html/cervix.html
2 Singh D, Vignat J, Lorenzoni V, *et al*. Global estimates of incidence and mortality of cervical cancer in 2020: a baseline analysis of the WHO global cervical cancer elimination initiative. *Lancet Glob Health* 2023;11:e197–206.
3 Gouy S, Morice P, Narducci F, *et al*. Prospective multicenter study evaluating the survival of patients with locally advanced cervical cancer undergoing laparoscopic para-aortic lymphadenectomy before chemoradiotherapy in the era of positron emission tomography imaging. *J Clin Oncol* 2013;31:3026–33.
4 Favre G, Guani B, Balaya V, *et al*. Sentinel lymph-node biopsy in early-stage cervical cancer: the 4-year follow-up results of the senticol 2 trial. *Front Oncol* 2020;10:621518.
5 Cibula D, McCluggage WG. Sentinel lymph node (SLN) concept in cervical cancer: current limitations and unanswered questions. *Gynecol Oncol* 2019;152:202–7.
6 Sponholtz SE, Mogensen O, Hildebrandt MG, *et al*. Sentinel lymph node mapping in early-stage cervical cancer - a national prospective multicenter study (SENTIREC trial). *Gynecol Oncol* 2021;162:546–54.
7 du Bois H, Heim TA, Lund AW. Tumor-draining lymph nodes: at the crossroads of metastasis and immunity. *Sci Immunol* 2021;6:eabg3551.
8 Heeren AM, Koster BD, Samuels S, *et al*. High and interrelated rates of PD-L1+CD14+ antigen-presenting cells and regulatory T cells mark the microenvironment of metastatic lymph nodes from patients with cervical cancer. *Cancer Immunol Res* 2015;3:48–58.
9 Balsat C, Blacher S, Herfs M, *et al*. A specific immune and Lymphatic profile characterizes the pre-metastatic state of the sentinel lymph node in patients with early cervical cancer. *Oncoimmunology* 2017;6:e1265718.
10 Chatterjee G, Pai T, Hardiman T, *et al*. Molecular patterns of cancer colonisation in lymph nodes of breast cancer patients. *Breast Cancer Res* 2018;20:143.
11 Grotz TE, Jakub JW, Mansfield AS, *et al*. Evidence of Th2 polarization of the sentinel lymph node (SLN) in Melanoma. *Oncoimmunology* 2015;4:e1026504.
12 Faghih Z, Rezaeifard S, Safaei A, *et al*. IL-17 and IL-4 producing CD8+ T cells in tumor draining lymph nodes of breast cancer patients: positive association with tumor progression. *Iran J Immunol* 2013;10:193–204.
13 Norouzian M, Mehdipour F, Ashraf MJ, *et al*. Regulatory and effector T cell subsets in tumor-draining lymph nodes of patients with squamous cell carcinoma of head and neck. *BMC Immunol* 2022;23:56.
14 van Krimpen A, Gerretsen VIV, Mulder EEAP, *et al*. Immune suppression in the tumor-draining lymph node corresponds with distant disease recurrence in patients with Melanoma. *Cancer Cell* 2022;40:798–9.
15 Quintana Á, Peg V, Prat A, *et al*. Immune analysis of lymph nodes in relation to the presence or absence of tumor infiltrating lymphocytes in triple-negative breast cancer. *Eur J Cancer* 2021;148:134–45.
16 Li YL, Hung WC. Reprogramming of sentinel lymph node microenvironment during tumor metastasis. *J Biomed Sci* 2022;29:84.
17 Kim T-J, Choi J-J, Kim WY, *et al*. Gene expression profiling for the prediction of lymph node metastasis in patients with cervical cancer. *Cancer Sci* 2008;99:31–8.
18 Cesano A. nCounter((R)) Pancancer immune profiling panel (Nanostring technologies, Inc., Seattle, WA). *J Immunother Cancer* 2015;3:42.
19 Wickham H. ggplot2: elegant Graphics for data analysis. New York Springer-Verlag; 2016.
20 Blighe K, Rana S, Lewis M. EnhancedVolcano: publication-ready volcano plots with enhanced colouring and labeling. R package version 1.18.0. 2023.
21 Bats A-S, Mathevet P, Buenerd A, *et al*. The sentinel node technique detects unexpected drainage pathways and allows nodal ultrastaging in early cervical cancer: insights from the multicenter prospective SENTICOL study. *Ann Surg Oncol* 2013;20:413–22.
22 Balaya V, Guani B, Morice P, *et al*. Long-term oncological safety of sentinel lymph node biopsy in early-stage cervical cancer: a post-hoc analysis of SENTICOL I and SENTICOL II cohorts. *Gynecol Oncol* 2022;164:53–61.
23 Lecuru FR, McCormack M, Hillemanns P, *et al*. SENTICOL III: an international validation study of sentinel node biopsy in early cervical cancer. a GINECO, ENGOT, GCIG and multicenter study. *Int J Gynecol Cancer* 2019;29:829–34.
24 Rotman J, Koster BD, Jordanova ES, *et al*. Unlocking the therapeutic potential of primary tumor-draining lymph nodes. *Cancer Immunol Immunother* 2019;68:1681–8.
25 Yaddanapudi K, Stamp BF, Subrahmanyam PB, *et al*. Single-cell immune mapping of melanoma sentinel lymph nodes reveals an actionable immunotolerant microenvironment. *Clin Cancer Res* 2022;28:2069–81.
26 Popeda M, Markiewicz A, Stokowy T, *et al*. Reduced expression of innate immunity-related genes in lymph node metastases of luminal breast cancer patients. *Sci Rep* 2021;11:5097.
27 Di Pilato M, Kfuri-Rubens R, Pruessmann JN, *et al*. CXCR6 positions cytotoxic T cells to receive critical survival signals in the tumor microenvironment. *Cell* 2021;184:4512–30.
28 Saiz-Ladera C, Baliu-Piqué M, Cimas FJ, *et al*. Transcriptomic correlates of immunologic activation in head and neck and cervical cancer. *Front Oncol* 2021;11:714550.
29 Balança C-C, Scarlata C-M, Michelas M, *et al*. Dual relief of T-lymphocyte proliferation and effector function underlies response to PD-1 blockade in epithelial malignancies. *Cancer Immunol Res* 2020;8:869–82.
30 Balança C-C, Salvioni A, Scarlata C-M, *et al*. PD-1 blockade restores helper activity of tumor-infiltrating, exhausted PD-1HiCD39+ CD4 T cells. *JCI Insight* 2021;6:e142513.
31 Patel SP, Othus M, Chen Y, *et al*. Neoadjuvant-adjuvant or adjuvant-only pembrolizumab in advanced Melanoma. *N Engl J Med* 2023;388:813–23.